The Hulse-Taylor pulsar 1913+16
—20 Apr 2010

Homework 6: Average 26/40

Ref: Taylor & Weisberg 1989, ApJ, 345, 434.
Taylor 1994, RMP 66.
Hulse 1994, RMP 66.

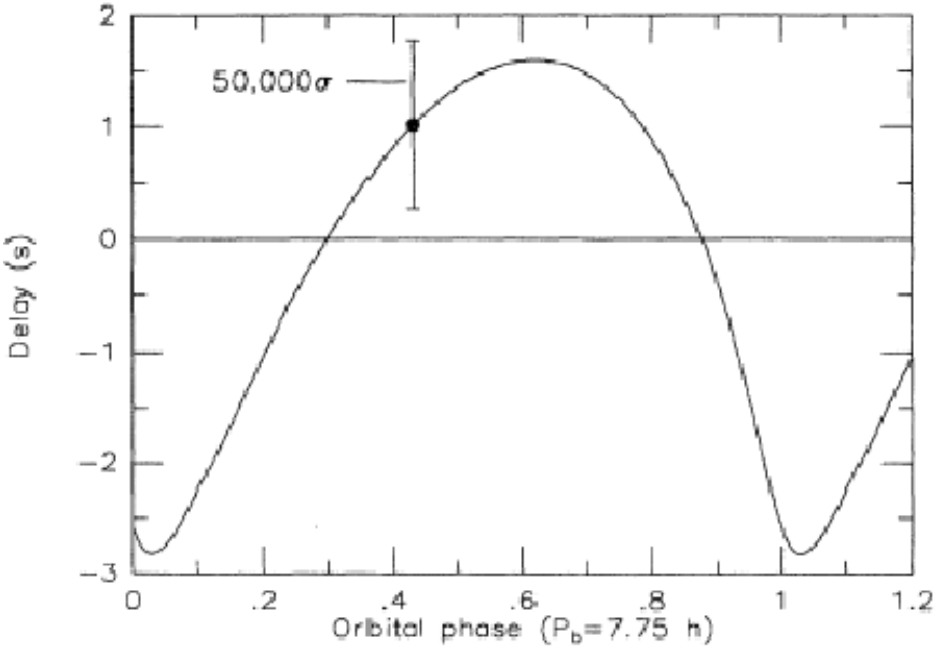

FIG. 5. Orbital delays observed for PSR 1913+16 during July, 1988. The uncertainty of an individual five-minute measurement is typically 50 000 times smaller than the error bar shown.
(Taylor 1994)

Period change

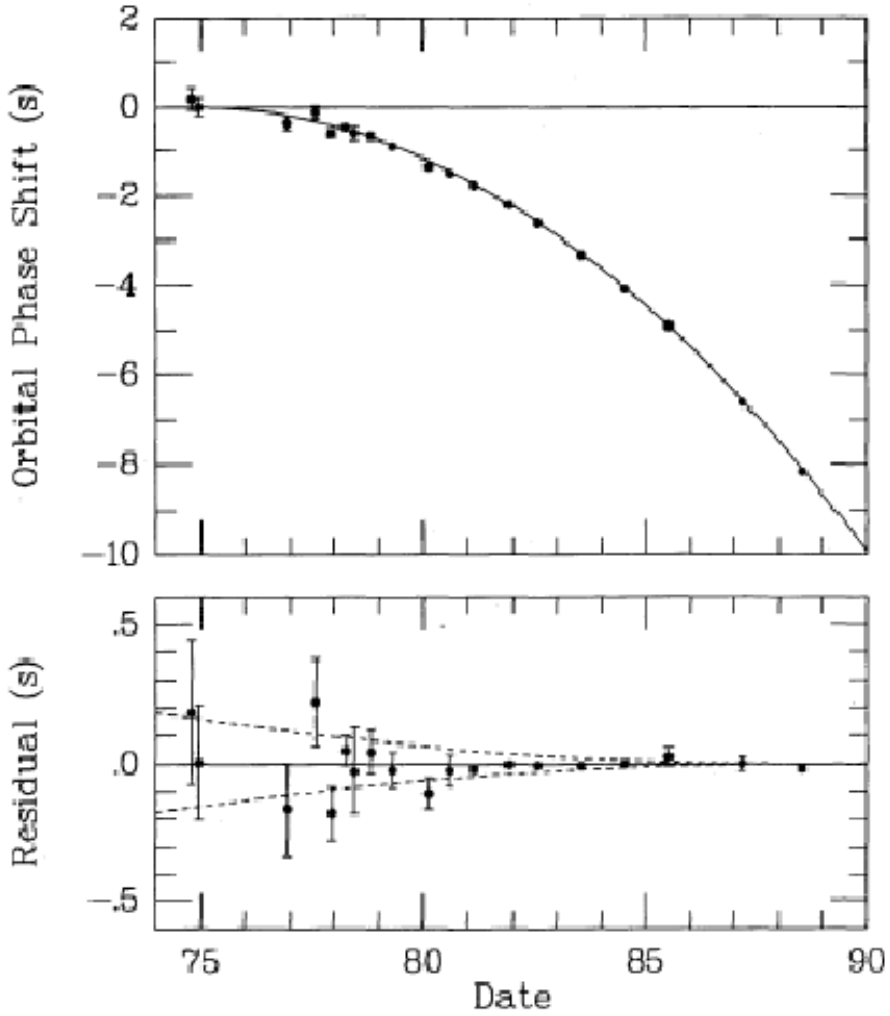

FIG. 5.-Top: Cumulative shift of the times of periastron passage relative to a nondissipative model in which the orbital period remains fixed at its 1974.78 value.
Bottom: Differences between the locally measured periastron times and those expected according to the DD(I) parameter set. Dashed curves illustrate differential trends that would be expected (relative to epoch 1988.54) if the rate of orbital decay $\dot{P}_b$ were 2% larger or 2% smaller. (Taylor & Weisberg)

Q: Why is the phase change (8s earlier in 1990 than in 1974)?

Results

$\dot{P}_b$ Period change due to gravitational radiation $\dot{P}_b \equiv \frac{dP}{dt} = -\frac{192}{5}\left(\frac{2\pi}{P}\right)^{5/3} m_1\, m_2\, M^{-1/3}\, f(\epsilon)$

γ Gravitational redshift and 2nd order Doppler effect $\gamma = \dfrac{e P_b G m_2 (m_1 + 2m_2)}{2\pi c^2 a_R M}$

$\dot{\omega}$ Precession of the periastron. $\dot{\omega} = 2\pi k / P_b$ $k = \dfrac{3GM}{c^2 a_R (1 - e^2)}$

$s = \sin i$ Inclination of the orbit

r amplitude of the Shapiro effect

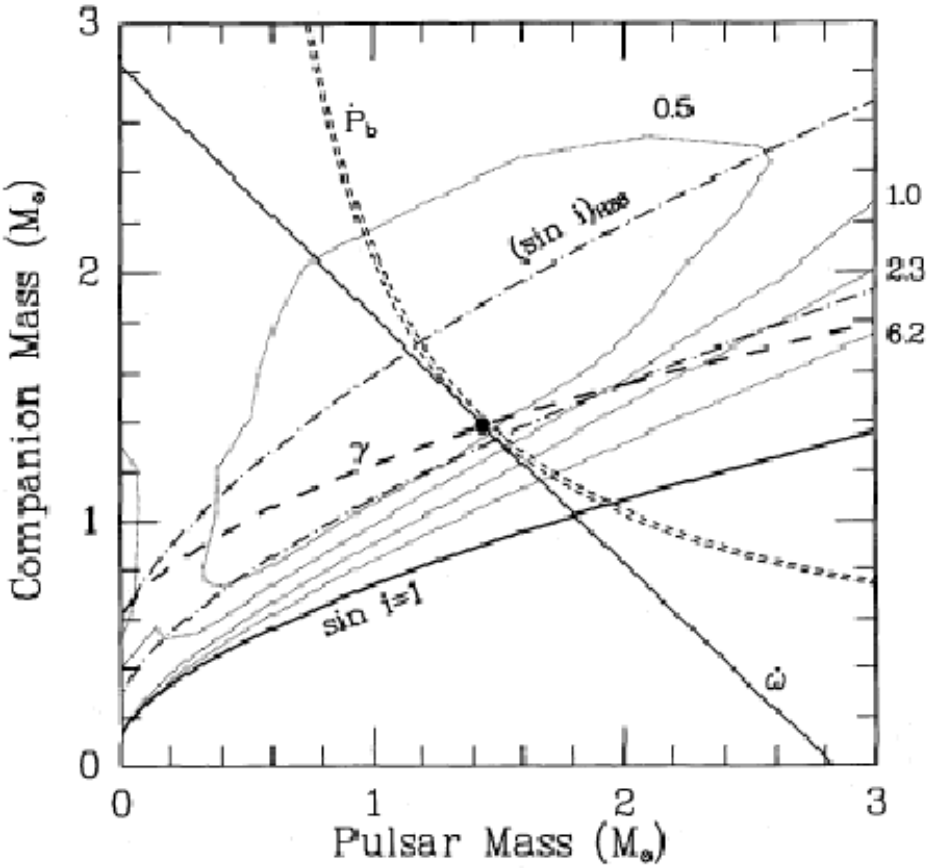

FIG. 9.-Restrictions on the pulsar mass, m1, and companion mass, m2, imposed by general relativity are indicated by curves labeled ω, γ', $\dot{P}_b$ and sin i_{OH88} (the Haugan 1988 sin i parameter). Uncertainties in ω and γ are smaller than the widths of their plotted curves; two curves are plotted for $\dot{P}_b$ and sin i_{OH88} bracketing the uncertainty range. Numerically labeled dotted curves represent a mapping of $\Delta\chi^2$ contours for parameters r and s from Fig. 7. Companion masses below the curve labeled sin i = 1 are incompatible with the mass function. The point marked with a filled circle corresponds to the mass values given for the DDGR solution in Table 5.
(Taylor & Weisberg)
Q: Write a one-sentence conclusion.

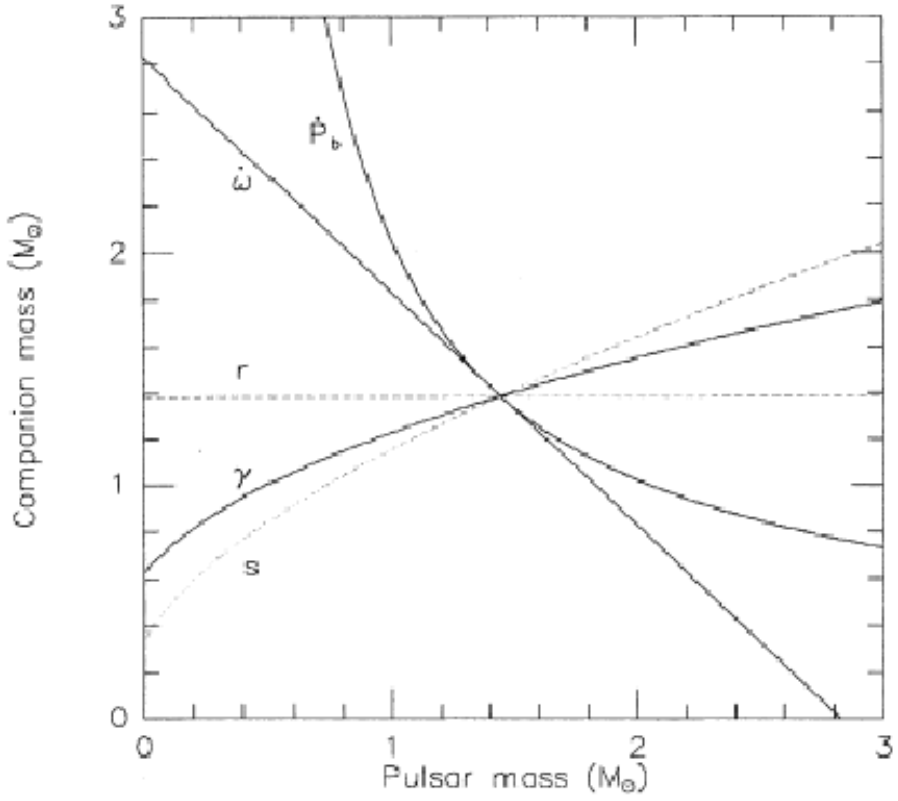

FIG. 11. Solid curves correspond to Eqs. (5)–(7) together with the measured values of $\dot{\omega}$, γ, and $\dot{P}_b$. Their intersection at a single point (within the experimental uncertainty of about 0.35% in $\dot{P}_b$), establishes the existence of gravitational waves. Dashed curves correspond to the *predicted* values of parameters r and s; these quantities should become measurable with a modest improvement in data quality.

(Taylor 1994)

Low-frequency gravity waves

Low-frequency gravity waves would change the distance between PSR1913+16 and us.
The lowest frequency detecable in the data is 10^{-12} Hz, which is 1/distance.

Q: What is the highest frequency gravity wave detectable by the data in Taylor & Weisberg? $1/\text{year} = 3\times10^{-8}$ Hz.

The limit is

$$\Omega_g < \frac{1}{2}\left(\frac{\delta \dot{P}_b}{P_b H_0}\right)^2 = 0.04 h^{-2}$$

Shapiro effect in 1855+09

From Taylor (1994) RMP.

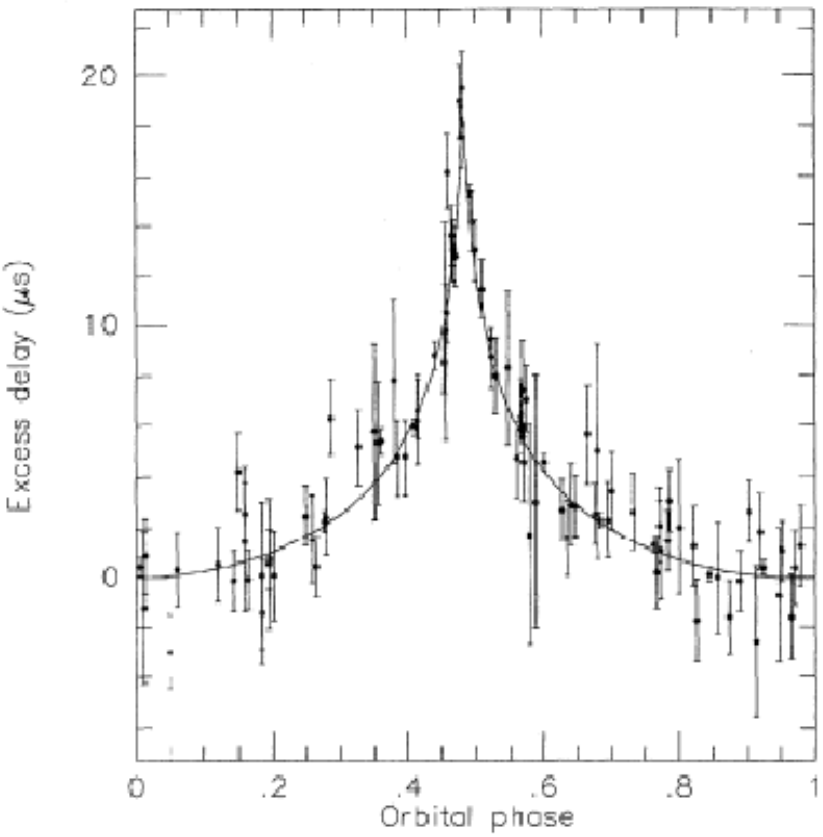

FIG. 8. Measurements of the Shapiro time delay in the PSR 1855+09 system. The theoretical curve corresponds to Eq. (10), and the fitted values of *r* and *s* can be used to determine the masses of the pulsar and companion star.